

Molecular Dynamics Study of the Proton Pump Cycle of Bacteriorhodopsin†

Feng Zhou, Andreas Windemuth, and Klaus Schulten*

Beckman Institute and Departments of Biophysics and Physics, University of Illinois at Urbana-Champaign, 405 North Mathews, Urbana, Illinois 61801

Received July 10, 1992; Revised Manuscript Received December 14, 1992

ABSTRACT: Retinal isomerization reactions, which are functionally important in the proton pump cycle of bacteriorhodopsin, were studied by molecular dynamics simulations performed on the complete protein. Retinal isomerizations were simulated in situ to account for the effects of the retinal–protein interactions. The protein structure employed was that described in Nonella et al. [Nonella, M., Windemuth, A., & Schulten, K. (1991) *Photochem. Photobiol.* 54, 937–948]. We investigated two mechanisms suggested previously for the proton pump cycle, the 13-cis isomerization model (C–T model) and the 13,14-dicis isomerization model. According to these models, retinal undergoes an all-trans \rightarrow 13-cis or an all-trans \rightarrow 13,14-dicis photoisomerization as the primary step of the pump cycle. From the simulations emerged a consistent picture of isomerization reactions and their control through the retinal–protein interactions which favors the 13,14-dicis isomerization model. Electrostatic interactions between the protonated Schiff base and its counterion are found to direct the stereochemistry of retinal in the photocycle: this and other interactions steer retinal toward the 13,14-dicis geometry in the primary photoreaction, toward the 13-cis geometry after its deprotonation, and to the all-trans isomeric form after its reprotonation. We also propose a catalytic mechanism involving hydrogen bonding of the Schiff base to main chain oxygen atoms of Val-49 and Thr-89 for the 13-cis \rightarrow all-trans thermal reisomerization of retinal. The all-trans \rightarrow 13-cis primary photoreaction required by the “C–T” model was found to be inhibited by the Schiff base–counterion interaction, but the possibility of such a reaction can not be excluded. In order to investigate the “C–T” model, we enforced an all-trans \rightarrow 13-cis photoisomerization in a simulation and monitored the subsequent protein conformational changes. The effects of internal water molecules on retinal isomerization reactions were studied by placing 16 water molecules in the proton conduction channel. The results indicate that water affects the nature of the Schiff base counterion and the nature of the primary photoreaction. Water chains, formed between positively and negatively charged protein groups in the proton conduction channel, are suggested to be involved in the reprotonation and deprotonation of retinal.

Bacteriorhodopsin (BR)¹ is a protein in the cellular membrane of *Halobacterium halobium* (Oesterhelt, 1973, 1976; Henderson, 1977) which acts as a light-driven proton pump transporting protons from the cytoplasmic side of the membrane to the extracellular side against a concentration gradient (Oesterhelt & Stoekenius, 1971; Racker & Stoekenius, 1974).

The light-absorbing chromophore of bacteriorhodopsin (BR₅₆₈) is *all-trans*-retinal (Harbison et al., 1985; Lin & Mathies, 1989), which is linked to Lys-216 through a protonated Schiff base. After light excitation of the chromophore, a pump cycle is initiated which involves several intermediates distinguishable through their absorption spectra (Lozier et al., 1975; Kouyama et al., 1988). During this cycle, retinal undergoes isomerization reactions and changes its protonation state such that one proton per absorbed photon is pumped. A widely adopted scheme of the photocycle is shown in Figure 1 (Lozier et al., 1975). A light-induced retinal isomerization occurs in the primary step of this cycle, the BR₅₆₈ \rightarrow J₆₂₅ transition, which proceeds within about 3 ps (Dobler et al., 1988; Mathies et al., 1988). The K₆₁₀ intermediate then relaxes into the L₅₅₀ intermediate. In the L₅₅₀ \rightarrow M₄₁₂ transition, the Schiff base proton is transferred from retinal to Asp-85 (Mogi et al., 1988; Braiman et al.,

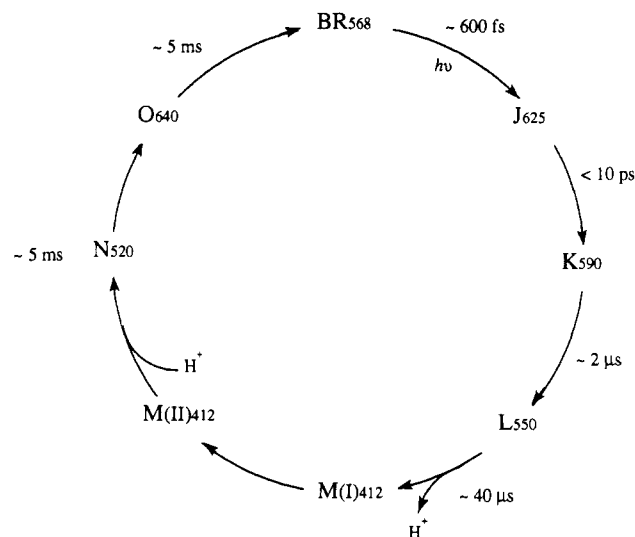


FIGURE 1: Widely adopted scheme of the photocycle of BR. A photon is absorbed by BR₅₆₈ in the primary photoreaction, and a proton is translocated from the cytoplasmic side to the extracellular side in the cycle. Two sequential M intermediates, M₁ and M₂, instead of a single intermediate M₄₁₂, are suggested by some experiments, e.g., in Váró and Lanyi (1991b).

1988; Gerwert et al., 1989; 1990) and is finally released to the extracellular side. Subsequently, retinal takes up another proton from the cytoplasmic side through Asp-96 during the M₄₁₂ \rightarrow N₅₂₀ transition (Gerwert et al., 1989; Holz et al., 1989; Otto et al., 1990). Finally, retinal reisomerizes to the

† This work was supported by a grant from the National Institutes of Health (P41RRO5969).

* To whom correspondence should be addressed.

¹ Abbreviations: BR, bacteriorhodopsin; MD, molecular dynamics; Lyr, lysine with the covalently bound retinal.

all-trans geometry, and the N_{520} intermediate relaxes back to BR_{568} through the O_{640} intermediate. The time needed for the transitions between different intermediates ranges from picoseconds to milliseconds. Recent reviews of the photocycle of BR are Khorana (1988), Birge (1990), and Mathies et al. (1991).

Several mechanisms for the proton pump cycle have been proposed, which can be classified into 13-cis (Fodor et al., 1988a) and 13,14-dicis (Schulten & Tavan, 1978; Schulten, 1978; Orlandi & Schulten, 1979; Schulten et al., 1984; Gerwert & Siebert, 1986) isomerization models according to the retinal geometry change postulated for the primary photoisomerization. The 13,14-dicis isomerization model suggests that retinal functions as a switch between a proton release pathway and a proton uptake pathway forming a proton donating/accepting complex within the protein. This model postulates a 13,14-dicis retinal configuration for L_{550} , with some conformational distortion in retinal which contributes to regulate the Schiff base pK_a . After the proton is released to Asp-85, a thermal isomerization of retinal to the 13-cis geometry brings the Schiff base nitrogen from contact with Asp-85 into contact with the reprotonation channel (Schulten, 1978). The 13,14-dicis model explains in a straightforward way also the transport of Cl^- ions in halorhodopsin (Oesterhelt et al., 1986) and possibly in BR (Dér et al., 1991).

The 13-cis isomerization models postulate a 13-cis retinal configuration for L_{550} . In these models the retinal geometry is essentially the same for the L_{550} , M_{412} , and N_{520} intermediates, and the proton pump is not controlled by changes in the retinal geometry but instead by a rearrangement of the protein. The "C-T" model is a 13-cis model which states that the protein can exist in two basic forms, T and C, corresponding to protein conformations accommodating the all-trans and 13-cis retinal geometries (Fodor et al., 1988a). The model suggests that, in the $L_{550} \rightarrow M_{412}$ transition, the Schiff base shuttles a proton to the exterior side through the primary proton acceptor Asp-85. Subsequently, the protein undergoes a conformational change from the T-form to the C-form. The protein conformational change thus serves as a switch disconnecting retinal from the extracellular side and connecting it to the cytoplasmic side. After this transition the Schiff base reprotonates from Asp-96, most likely indirectly through a hydrogen-bonded chain (Nagle & Nagle, 1983; Braiman et al., 1988; Papadopoulos et al., 1990; Gerwert, 1992).

Unfortunately, the exact isomeric states of retinal in K_{610} and L_{550} are not known, and it is not possible yet to discriminate between the two models through direct observations. Experimental results and quantum-chemical investigations appear to be consistent with a 13-cis geometry (Smith et al., 1986; Fodor et al., 1988b) as well as with a 13,14-dicis geometry (Gerwert & Siebert, 1986; Fahmy et al., 1989; Grossjean et al., 1989) for the L_{550} intermediate. Quantum chemical calculations have shown that properties of the protonated Schiff base such as its electronic absorption spectrum (Nakanishi et al., 1980; Baasov & Sheves, 1985), torsional barriers (Orlandi & Schulten, 1979; Schulten et al., 1984; Oesterhelt et al., 1986), and vibrational frequencies (Baasov & Sheves, 1984a; Grossjean et al., 1990) can be influenced strongly by charged groups in the vicinity of the conjugated system as well as by the protonation state of retinal Schiff base, which makes an unequivocal assignment of the retinal geometry from vibrational frequencies very difficult. However, a 13-cis geometry of retinal has been determined unequivocally in the M_{412} state of the photocycle in which retinal

is deprotonated and less affected by electrostatic interactions (Pettei et al., 1977; Aton et al., 1977).

In Nonella et al. (1991), an equilibrated structure of BR with loop regions has been constructed using molecular dynamics simulations starting from the Henderson structure (Henderson et al., 1990), i.e., from the best 3-D structure available at this time. The study reported in Nonella et al. (1991) also showed that a retinal 13,14-dicis photoisomerization is significantly favored over a 13-cis photoisomerization by the retinal-protein interaction. The tight packing of retinal in the protein matrix was suspected to be the dominant factor which makes the less space demanding 13,14-dicis isomerization more favorable, although it was not explained why a 13-cis isomerization could not be accommodated through rotation of the flexible lysine side chain.

In the present paper, we extend the study in Nonella et al. (1991) by further investigating the primary photoisomerization reaction. We show that the electrostatic interaction between the protonated Schiff base and its counterion is also a crucial factor for the preference of a 13,14-dicis photoisomerization over a 13-cis photoisomerization. We also study the thermal isomerization reactions in the photocycle, namely, the 13,14-dicis \rightarrow 13-cis isomerization and the 13-cis \rightarrow all-trans isomerization which retinal undergoes during the $N_{520} \rightarrow O_{640}$ transition (Smith et al., 1983).

Below we will also consider how the protein could possibly accommodate a 13-cis photoisomerization which, according to the "C-T" model, is the primary reaction step. For this purpose we enforced a corresponding primary photoreaction.

In order to explain the stability of the Schiff base-counterion complex and the high pK_a value of the Schiff base in BR, it was suggested that the Schiff base-counterion complex is in a rather hydrophilic environment where protein dipoles (Warshel & Barboy, 1982) or residual waters (Sandorfy & Vocelle, 1986; Baasov & Sheves, 1986) could solvate the ion pair. Later experiments (Hildebrandt & Stockburger, 1984; Papadopoulos et al., 1990) further suggest there are about 10 water molecules in BR and a few of them might be directly hydrogen-bonded to the Schiff base. Models have been proposed that water molecules participate in forming a complex counterion for the Schiff base (de Groot et al., 1990; Needleman et al., 1991). Water molecules are also functionally important in the proton pump cycle. Dehydrated BR forms a slowly decaying M intermediate which returns to BR_{568} (Váró & Keszthelyi, 1983), and the conformational change in the $M_1 \rightarrow M_2$ transition does not occur (Braiman et al., 1987). Water structure changes have also been observed during the photocycle (Maeda et al., 1992b). Therefore, it appears that internal water molecules are important in the Schiff base-counterion interaction and are necessary for the reprotonation of retinal from Asp-96. Unfortunately, the resolution of the Henderson structure is not high enough to precisely determine the position of the internal water. Nevertheless, we placed water molecules into the proton conduction channel at various sites in order to study the role of internal water in the BR photocycle. The results suggest that water can affect the nature of the Schiff base counterion as well as the retinal isomerization reactions, leaving the 13,14-dicis photoisomerization and the 13,14-dicis \rightarrow 13-cis isomerization after retinal deprotonation energetically favorable. In our simulations, water molecules were also found to form hydrogen-bonded chains in the proton conduction channel of the cytoplasmic side, which may serve as "proton wires" for the proton transfer from and to the retinal Schiff base (Nagle & Nagle, 1983).

MATERIALS AND METHODS

The calculations in the first part of this paper are performed in vacuum on a complete structure of BR (Nonella et al., 1991) derived from the structure provided by Henderson (Henderson et al., 1990) for the helical part of the protein. The structures from Henderson et al. (1990) and Nonella et al. (1991) match well, the root-mean-square deviation of the backbone atoms of the helical portion being 2.85 Å. This deviation is small compared to the resolution of the Henderson structure, namely, 3.5 Å in a direction parallel to the membrane plane and 10 Å in the perpendicular direction. The relative positions of the transmembrane helices are rearranged slightly compared to the Henderson structure. Helix G is found to move very little in a rms fitted comparison of the equilibrated structure and the Henderson structure. Helix D moves about 2 Å toward the cytoplasmic side. Other helices move by similar magnitudes in random directions.

The protonation states of titratable groups in BR₅₆₈ were assumed as described in Nonella et al. (1991), i.e., using the standard protonation states as stated in the X-PLOR topology and parameter file *param19* (Brünger, 1988) with the exception of Asp-96 and Asp-115, which were assumed to be protonated, in accordance with experimental observations (Gerwert et al., 1989; Engelhard et al., 1990). An important deviation from the structure in Nonella et al. (1991) was a change of the position of Arg-82 toward the cytoplasmic side of BR; we adopted this new position since it had been suggested that residues Asp-85, Arg-82, and Asp-212 form a proton-accepting complex on the extracellular side of retinal (Mogi et al., 1988; Braiman et al., 1988; Gerwert et al., 1990; Otto et al., 1990; Dér et al., 1991). Recent electrostatic calculations also support the repositioning of Arg-82 (Bashford & Gerwert, 1992). An additional MD simulation of 10 ps was performed to equilibrate the corresponding BR structure. In the resulting structure, e.g., shown in Figure 4 (see below), Arg-82 is in the vicinity of Asp-85 and Asp-212 and is a counterion of both acidic groups. The direct counterion of the protonated Schiff base is Asp-212 in this equilibrated structure, whereas Asp-85 is approximately 2 Å farther away from the Schiff base as compared to the Henderson structure. This arrangement of the Schiff base counterion is not consistent with the experimental evidence that Asp-85, instead of Asp-212, is the primary proton acceptor from the Schiff base (Mogi et al., 1988; Braiman et al., 1988; Gerwert et al., 1989, 1990). However, such an arrangement of Asp-85 and Asp-212 is observed in all our test simulations of BR in vacuum. The simulated protein was stable during a total simulation time of more than 300 ps. In the second part of this paper, we placed explicit water molecules in the retinal binding pocket (described below), and the nature of the Schiff base counterion in the equilibrated structure was changed to a hydrogen-bonding complex formed by water, Asp-85, Asp-212, and Arg-82, water molecules being the direct counterion of the protonated Schiff base.

All dynamics simulations presented below were carried out using the program X-PLOR (Brünger, 1988), which implements the CHARMM (Brooks et al., 1983) force field. Partial charges for the protonated and unprotonated Schiff base have been used as determined using the program ZINDO (Ridley & Zerner, 1973). Force constants for retinal were derived from molecules with similar chemical structures for which parameters are available in CHARMM and X-PLOR. The united atom model was used for the BR structure, and no explicit hydrogen bond energy was included. A distance cutoff

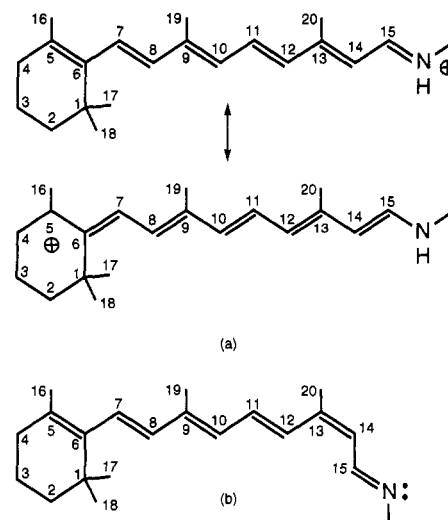


FIGURE 2: Schematic model for (a) all-trans protonated retinal and (b) 13-cis unprotonated retinal. The photoisomerization around the 13–14 bond, and possibly the 14–15 bond, is functionally important in the proton pump cycle of BR (Fodor et al., 1988a; Schulten, 1978). The figure shows that protonation induces an admixture of resonance structures which weakens double bonds and strengthens single bonds.

Table I: List of Partial Charges Used in Our Simulations for the Atoms of the Retinal Chromophore^a

atom	protonated	unprotonated	atom	protonated	unprotonated
N	-0.35	-0.35	C6	-0.029	-0.026
H	0.25	0.25	C7	0.037	-0.008
C _α	0.1	0.1	C8	-0.022	-0.016
C _β	0.0	0.0	C9	0.059	0.009
C _γ	0.0	0.0	C10	-0.036	-0.029
C _δ	0.0	0.0	C11	0.087	0.006
C _ε	0.221	0.128	C12	-0.021	-0.007
N(SB)	-0.509	-0.406	C13	0.104	0.023
H(SB)	0.519		C14	-0.030	-0.007
C	0.55	0.55	C15	0.331	0.194
O	-0.55	-0.55	C16	0.042	0.023
C1	0.057	0.059	C17	-0.004	-0.008
C2	0.006	-0.005	C18	-0.004	-0.008
C3	0.011	0.0	C19	0.059	0.032
C4	0.047	0.026	C20	0.059	0.037
C5	0.016	-0.017			

^a N(SB) and H(SB) denote the Schiff base nitrogen and proton, respectively. Charges were calculated using the quantum chemistry program ZINDO (Ridley & Zerner, 1973) separately for both protonated and unprotonated retinal in the all-trans state.

of 8.0 Å was used for nonbonded interactions, and the dielectric constant used was 1.0.

The geometry of retinal in BR₅₆₈ was assumed to be all-trans (Lin & Mathies, 1989). The models for the all-trans protonated retinal and the 13-cis unprotonated retinal are shown in Figure 2. The torsional barriers for the 13–14 double bond and 14–15 single bond were chosen according to the quantum chemical calculations reported in Schulten (1978) and Schulten et al. (1984). For the protonated retinal, the torsional barriers were taken to be 20 kcal/mol for both the double bonds (including the 13–14 bond) and the single bonds (including the 14–15 bond). In deprotonated retinal, the torsional barriers of the single and double bonds are changed due to the redistribution of electrons along the conjugated system; we chose barriers of 47 kcal/mol for the double bonds and of 2 kcal/mol for the single bonds. Deprotonation of retinal also causes changes in atomic partial charges. The partial charges of protonated and deprotonated retinal chosen are given in Table I.

The potential which according to the X-PLOR force field governs the motion of dihedral angles is

$$E_{\text{dih}}(\phi) = k_{\text{dih}}[1 + \cos(n\phi + \delta)], \quad (1)$$

with $n = 2$ (periodicity), $k_{\text{dih}} = 10$ kcal/mol (half of the torsional barrier), and $\delta = 180^\circ$ (phase factor) for the 13–14 bond in the case of the planar, all-trans retinal chain conformation. The photoisomerization has been induced by abruptly changing the torsional potential in eq 1 for the 13–14 bond such that the all-trans conformation became unstable and the respective cis-conformation stable. During the photoisomerization, the potential adopted for 13–14 bond was accordingly

$$E_{\text{dih}}^{13}(\phi) = k_{\text{dih}}^{13}(1 - \cos \phi) \quad (2)$$

This potential has a maximum at the all-trans position $\phi = 180^\circ$ and a minimum at the cis position $\phi = 0^\circ$. k_{dih}^{13} is taken as 23.5 kcal/mol such that the torsional potential at its maximum measures 47 kcal/mol, which is close to the energy of a 568-nm photon.

The primary reaction of the photocycle is very fast. The time needed to reach the intermediate J_{625} is only 0.5 ps (Dobler et al., 1988; Mathies et al., 1988). This implies that the crossing between the potential energy surfaces of the S_0 and S_1 states of retinal occurs close to the maximum of the ground state potential surface (Schulten, 1978). It is suggested that retinal relaxes to the excited state minimum near the ground state isomerization barrier, with a $\sim 90^\circ$ torsion for the 13–14 bond, in about 200 fs (Mathies et al., 1991) and then crosses to the ground state potential surfaces where the photoisomerization is completed. In our simulations this process was described by the single potential surface (eq 2) which, hence, represents in its higher energy range the excited state and in its lower energy range the ground state potential. Photoisomerization of the 13–14 bond is achieved by placing the initial all-trans state at the maximum of eq 2. Subsequent simulations then monitor the relaxation of retinal down the surface (eq 2). The simulations include the effect of the resistance that the protein poses to the isomerization reaction enforced by potential (eq 2).

We started the simulated photoisomerization from the all-trans state. Since the behavior of the 14–15 bond is essential for the resulting retinal geometry, and since little is known regarding the torsional barrier for this bond, we carried out simulations with different barriers for this bond. The potential describing the torsional angle of the 14–15 bond is

$$E_{\text{dih}}^{14}(\phi) = k_{\text{dih}}^{14}[1 - \cos(2\phi + 180)] \quad (3)$$

where the parameter k_{dih}^{14} is chosen according to the torsional energy barrier desired. In one simulation, we chose a torsional barrier (of the 14–15 single bond) of 2 kcal/mol, to enable essentially free rotation around this bond such that both the all-trans \rightarrow 13-cis and the all-trans \rightarrow 13,14-dicis isomerizations are possible. In another simulation, we enforced the all-trans \rightarrow 13-cis isomerization by assuming a barrier of 10 kcal/mol preventing rotation around the 14–15 bond. All simulations, except where otherwise stated, were performed at 300 K.

Thermal isomerizations of retinal upon deprotonation and reprotonation were also studied. In order to describe the proton transfer processes in the photocycle, we modified the protonation states of retinal between simulations. To model retinal's deprotonation, we deprotonated the Schiff base and protonated the primary proton acceptor Asp-85. To model retinal's

reprotonation, we protonated the Schiff base and deprotonated the proton donor Asp-96.

During the photocycle, changes in side group protonation states and in the geometry of retinal should cause protein conformational changes between different intermediates, which have been experimentally observed (Becher & Ebrey, 1978; Glaeser et al., 1986; Dencher et al., 1989; Maeda et al., 1992a,b). Although it is impossible to describe these conformational changes accurately on the basis of picosecond time scale simulations, we still consider it meaningful to study the photocycle by simulating the possible retinal isomerization reactions starting from the structures and protonation states described above. First, properties of retinal should be mainly sensitive to the protein groups in its vicinity but should be rather insensitive to global protein conformation. Second, experiments have shown that bacteriorhodopsin is rather rigid during the photocycle (Glaeser et al., 1986), and the conformational changes should be mainly due to retinal and due to a few residues in the vicinity of retinal's binding site. MD simulations are likely to rearrange these residues correctly in a few picoseconds after one changes the protein protonation state mimicking the actual proton transfer processes in the photocycle, provided that the conformational changes in the protein backbone are small.

To simulate retinal thermal reversion to the all-trans state, the torsional barrier of the 13–14 double bond was lowered to different values, some artificially small. The low barriers made it possible that the isomerization reaction is realized in simulations which can only cover a few hundred picoseconds of real time. The simulations should provide information on the influence of steric and electrostatic interactions as on the isomerizations but do not provide information on the time scale of the reaction. Detailed explanations of the various parameters used are given under Results.

At the last stage of the present work, we explored the possible effects of the internal water molecules on the BR photocycle. The TIP3P water model (Jorgenson et al., 1983) was used for the water molecules. In the Henderson structure, the distance between Asp-96 and the Schiff base is about 12 Å, and it is suggested that 3–4 water molecules are involved in the reprotonation of retinal from that side group. Therefore, four water molecules were placed at random inside the hydrophobic channel on the cytoplasmic side. The channel on the extracellular side is more hydrophilic, and neutron diffraction observations suggest there are at least four tightly bound water molecules near the Schiff base (Papadopoulos et al., 1990). We placed six water molecules around the Schiff base-counterion complex. Six further water molecules were also placed near the extracellular surface of the protein. To obtain a better model of the ionic groups around the Schiff base, including Asp-85, Asp-212, Arg-82, and the water molecules, we first protonated Asp-85 and Asp-212 and equilibrated the structure for 20 ps at 300 K. Asp-85 and Asp-212 were then reprotonated, and the structure was equilibrated for 80 ps at 300 K. Such a procedure was used because BR₅₆₈ is formed from the O₆₄₀ intermediate in which Asp-85 and Asp-212 are suggested to be protonated (Gerwert et al., 1990; Gerwert, 1992; Gerwert & Souvignier, 1992).

RESULTS

The 13,14-dicis Isomerization Model

The Primary Photoisomerization. We simulated the photoisomerization by instantaneously changing the torsional potential of the 13–14 bond as described under Materials and

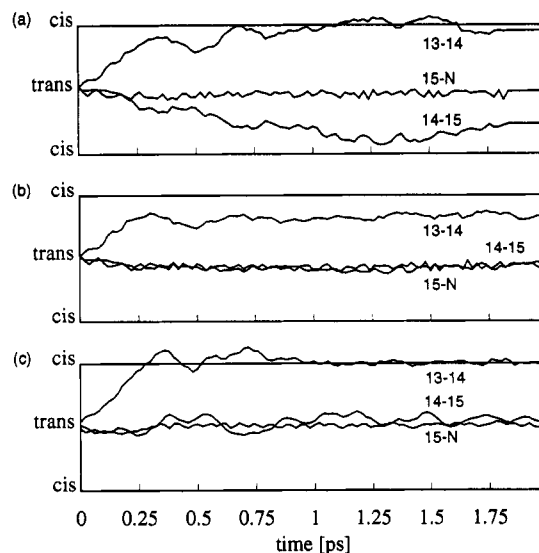


FIGURE 3: Dihedral angles (designated by their respective bonds) of retinal during simulations A1 [top (a)], A2 [middle (b)] and A3 [bottom (c)]. A torsional barrier of 2 kcal/mol for the 14–15 bond has been chosen in simulation A1 and a torsional barrier of 10 kcal/mol in simulation A2. Retinal has been protonated in both simulation A1 and A2. In simulation A3 retinal has been unprotonated, and a torsional barrier of 2 kcal/mol for the 14–15 bond has been assumed.

Methods. We carried out two simulations, simulation A1 with a torsional barrier of 2 kcal/mol for the 14–15 single bond and simulation A2 with a barrier of 10 kcal/mol for this bond. Both simulations were started from the all-trans structure and lasted 7 ps. The resulting structures were both equilibrated for 2 ps using the torsional potentials for protonated retinal in the ground state.

Figure 3a presents the time dependence of the dihedral angles of the 13–14, 14–15, and 15–N bonds in simulation A1. The photoisomerization is found to be completed after about 1.2 ps. In addition to the isomerization around the 13–14 bond enforced by potential (eq 2), a concomitant rotation of approximately 140° around the 14–15 bond occurs. After 2 ps of equilibration of the resulting structure, applying the ground state torsional potentials for retinal, the isomerization around the 14–15 bond is complete, and retinal remains in a 13,14-dicis geometry.

Figure 4 compares the conformation of all-trans retinal and of 13,14-dicis retinal after the isomerization induced in simulation A1. The retinal plane is twisted after the isomerization reaction. The twist induced in retinal after the primary photoreaction could explain the intense hydrogen out of plane modes in the resonance Raman and FTIR spectra of the K intermediate (Mathies et al., 1991). During the isomerization, the C_{10} – C_{15} atoms of retinal move toward the cytoplasmic side of the protein. The magnitude of the movement is about 1.7 Å for the C_{15} atom and 2–3 Å for the C_{13} , C_{14} , and C_{20} atoms. Because of the positive partial charges on these carbon atoms, this movement corresponds roughly to a 1-Å movement of a unit positive charge toward the cytoplasmic side.

Figure 3b presents the time dependence of the dihedral angles of the 13–14 and 14–15 bonds within the first 2 ps of simulation A2. Rotation around the 14–15 bond is hindered by a torsional barrier of 10 kcal/mol in this simulation. In this case, the trans \rightarrow cis isomerization of the 13–14 bond is impeded and is not completed within 7 ps. Retinal is brought into a highly twisted 13-cis conformation after the simulation; the dihedral angle of the 13–14 bond is approximately 60° .

After a 2-ps equilibration with the ground state potential, the structure relaxed back to the original all-trans conformation (not shown). It is worth noting that in both simulations A1 and A2 the Schiff base proton moves very little and remains hydrogen bonded to the counterion Asp-212. No major protein conformational changes were observed during both isomerizations A1 and A2.

The importance of the Schiff base-counterion interaction for retinal's stereochemistry in the primary photoreaction is proven in simulation A3, in which a photoisomerization for the *unprotonated* all-trans retinal was induced. The isomerization reaction was induced using the same dihedral potentials as in simulation A1. The trajectory of the relevant dihedral angles in simulation A3 is presented in Figure 3c. Retinal is seen to undergo a 13-cis isomerization instead of the 13,14-dicis isomerization of simulation A1.

It is not shown in simulations A1, A2, and A3 how the retinal isomerization reaction would be affected if the direct counterion of the Schiff base is Asp-85 instead of Asp-212 which is assumed here. It is very likely that an alternative anionic counterion (Asp-85) would exert very similar effects on the isomerization of retinal due to a similar Coulombic interaction with the Schiff base. Further simulations described later in this paper, where a more likely Schiff base counterion is formed when explicit water molecules are placed in the retinal binding pocket, will address this problem more directly.

We also investigated the role of the lysine (Lys-216) side chain during the primary photoisomerization. Experimental evidence exists that the lysine side chain undergoes a conformational change during the $BR_{568} \rightarrow L$ transition (Gat et al., 1992), but it is not clear whether such a conformational change has any effect on the nature of the retinal isomerization reaction. For rhodopsin, experiments have shown that this protein remains functional when the retinal-bound lysine is mutated to Ala or Gly and the chromophore is given in the form of a Schiff base with an *n*-alkylamine (Zhukovsky et al., 1991). These experiments suggest that the covalent attachment of the chromophore to the protein backbone is not important for the function in the case of rhodopsin. To investigate the function of the lysine side chain for the retinal isomerization in BR, we cleaved the lysine chain in simulation A1 between the C_α and C_β atoms of Lys-216 by setting the force constant of all the energy terms involving this bond to zero, assuming otherwise the same conditions as in simulation A1 (see above). The simulation covered 2 ps. We found that retinal undergoes a 13,14-dicis isomerization within 1.2 ps (not shown) demonstrating that the covalent attachment of retinal to the protein matrix does not affect the isomerization reaction significantly. The lysine side chain undergoes only small conformational changes in simulations A1 and A3; however, a larger conformation change is observed in simulation A2 where a 13-cis isomerization occurred.

The 13,14-dicis \rightarrow 13-cis Isomerization. The 13,14-dicis model implies that there exist, in the proton pump cycle of BR, two M intermediates, M_1 and M_2 of unprotonated retinal in the 13,14-dicis and 13-cis state, respectively (Schulten et al., 1984), though the M_1 intermediate might be too short-lived to be observed. Indeed, the existence of two consecutive M states has also been concluded from an analysis of the photocycle kinetics (Váró & Lanyi, 1990). The explanation of the intermediates is that retinal transfers its Schiff base proton to Asp-85 in the $L_{550} \rightarrow M_1$ transition and enables retinal to undergo a 13,14-dicis \rightarrow 13-cis isomerization, which corresponds then to the $M_1 \rightarrow M_2$ transition. An important aspect of the 13,14-dicis \rightarrow 13-cis isomerization is the change

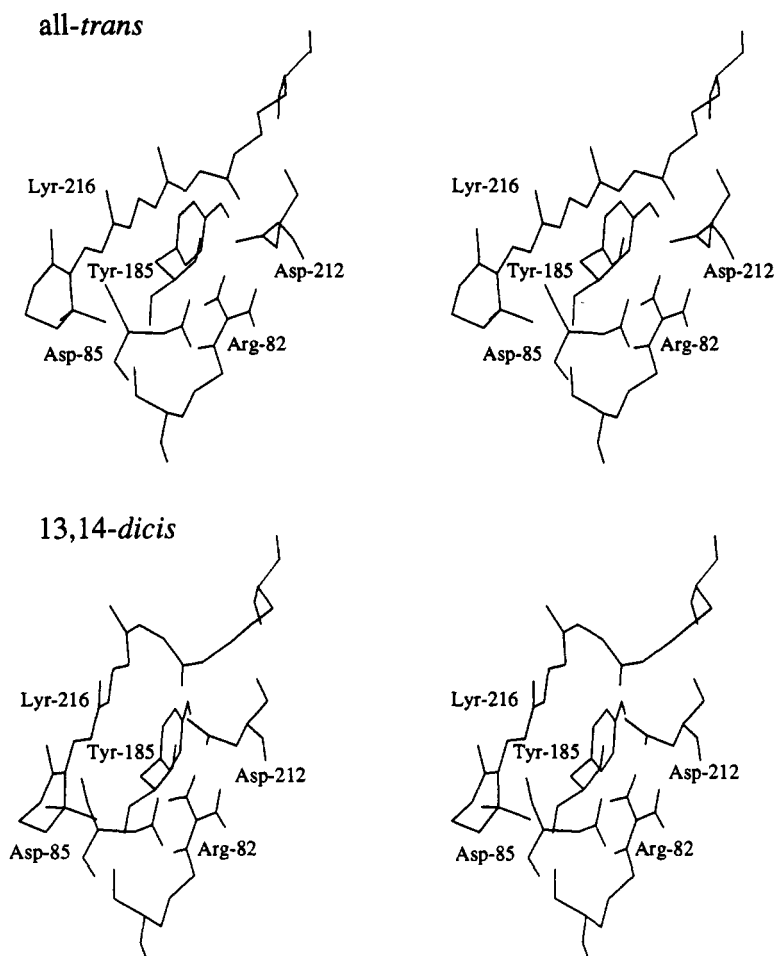


FIGURE 4: Stereoviews of retinal before (top) and after (bottom) the isomerization reaction as described by simulation A1. Neighboring residues Asp-85, Arg-82, Asp-212, and Tyr-185 are also shown.

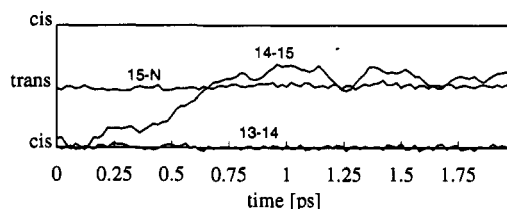


FIGURE 5: Dihedral angles (designated by their respective bonds) of retinal during the initial 2 ps of simulation B1. Retinal is deprotonated and Asp-85 protonated at the start of the simulation.

of the position of the Schiff base nitrogen from a site in contact with the proton acceptor Asp-85 on the extracellular side to a new site in contact with the proton donor on the cytoplasmic side.

In order to investigate the question of whether the suggested retinal isomerization occurs spontaneously upon deprotonation, we started from the 13,14-dicis structure generated by simulation A1 which had been equilibrated for 2 ps. Asp-85 was protonated, and partial charges and dihedral potentials of retinal were changed to those of the unprotonated chromophore as described under Materials and Methods. Simulation B1 was then carried out for 2 ps. Figure 5 presents the time dependence of the dihedral angles of the 13–14, 14–15, and 15–N bonds in the simulation. Retinal is seen to undergo a 13,14-dicis \rightarrow 13-cis isomerization. The time needed to complete this reaction is only 700 fs. The occurrence of the 700-fs isomerization is due to two factors. First, the torsional barrier for the 14–15 bond is reduced in the unprotonated retinal; second, deprotonation of retinal releases

the Coulomb interaction between the Schiff base and its counterion, enabling essentially free rotation of the 14–15 bond. It should be noted that the fast isomerization around the 14–15 bond implies that the intermediate M_1 , i.e., the primary unprotonated form of the chromophore of BR's pump cycle, should be very short lived, and, hence, might not be observable.

The 13-cis Isomerization Model

The $BR_{568} \rightarrow J \rightarrow K$ Transition. Although our simulations indicate that an all-trans \rightarrow 13-cis photoisomerization is severely hindered in BR, we also investigated how the protein and retinal could possibly accommodate such a reaction. For this purpose we enforced an all-trans \rightarrow 13-cis isomerization in simulation C1 by choosing for k_{dih}^{13} (eq 2) a value of 47 kcal/mol, thus assuming storage of 94 kcal/mol of energy in the photoexcited trans state of the 13–14 bond. This energy exceeds the energy of electronic excitation of retinal and, hence, appears unphysical. However, such large value of k_{dih}^{13} was required to ensure the successful completion of the desired isomerization. In simulation C1, k_{dih}^{14} (eq 3) was assumed to be 5.0 kcal/mol (the torsional barrier assumed is thus 10.0 kcal/mol) to prevent rotation around the 14–15 bond. The simulation was carried out for 20 ps. Such long simulation time was necessary since the 13-cis product state relaxes back to the all-trans form if simulation C1 is terminated too early and the ground state torsional potential applied. In simulation A2, where a value of 47 kcal/mol was chosen for k_{dih}^{13} , the 13-cis product cannot be stabilized within 7 ps. The reader should note that such a long time range for the altered potential

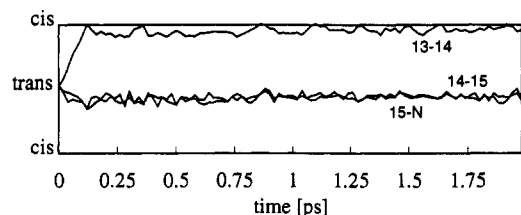


FIGURE 6: Dihedral angles (designated by their respective bonds) of retinal during the initial 2 ps of simulation C1. The torsional barrier of the 14–15 bond is taken as 10 kcal/mol in this simulation, and the potential energy of the trans state of the 13–14 bond is assumed to be higher than that of the cis state by 94 kcal/mol to ensure a complete 13-cis isomerization.

describing the excited states of retinal is in conflict with the observation that the thermally stable J intermediate forms within only 500 fs (Dobler et al., 1988; Mathies et al., 1988).

The dihedral angle trajectories during simulation C1 are presented in Figure 6. Retinal is seen to undergo an almost complete 13-cis isomerization within 200 fs in simulation C1. This isomerization is accomplished by a motion which brings the Schiff base proton closer to the main chain oxygen atom of Asp-212 but leaves it within 4 Å from the Asp-212 carbonyl group. The 14–15 and 15–N bonds of retinal become twisted (with torsion angles around 140°), but the remaining part of retinal remains quite planar immediately after this motion.

Retinal, still being subject to the modified potential (eq 2), subsequently diminished its twist around the Schiff base bond through an overall rotation by approximately 45°, the motion taking about 3 ps. The rotation is smaller for the β -ionone ring which is tightly packed in the protein, and the originally planar retinal becomes twisted. Such a twist also has been observed for retinal after the 13,14-dicis isomerization. Bending and subsequent rotation of retinal in the 13-cis isomerization caused the β -ionone ring to protrude toward helix D, whereas the C₉–C₁₃ atoms protruded toward helix G [nomenclature of helices according to Henderson et al. (1990)]. Within the remaining 17 ps of simulation C1, the Schiff base proton vacillates between the main chain oxygen and the carbonyl group of Asp-212 as counterions. The distance between the Schiff base proton and the carbonyl group is about 1 Å larger compared to the structure before isomerization and corresponds to a small movement of positive charge toward the cytoplasmic side.

Experimental studies of the primary photoreaction have shown that BR first forms a J intermediate within 500 fs and relaxes then to the K intermediate on a 3-ps time scale (Dobler et al., 1988). Since simulation C1 gives similar reaction times for retinal isomerization and relaxation, one may conclude that these processes might correspond to the BR₅₆₈ → J and J → K transitions. The structures of the putative J and K intermediate obtained in simulation C1 are shown in Figure 7.

The K → L Transition. To investigate how retinal could further relax and produce a more planar 13-cis chromophore in the K → L transition, simulation C2 was carried out for 20 ps at $T = 400$ K starting from the structure obtained in simulation C1 but assuming the ground state potential (eq 1) for the protonated Schiff base retinal.

A further rotation of retinal, mainly in the β -ionone ring region, occurred within about 13 ps. This motion left retinal almost parallel to the membrane surface and decreased the twist of the retinal plane. In order to allow such a rotation, a conformational rearrangement occurred to helix D. Met-118, which is originally in contact with the β -ionone ring, moved out of the binding pocket, whereas Asp-115 moved

into the binding pocket close to the β -ionone ring. Most of the aromatic residues in the binding pocket were also affected by retinal's relaxation and shifted by 1–2 Å to produce a better packing around the relaxed retinal. After the relaxation, the twist of retinal plane was reduced, and the Schiff base was again hydrogen bonded to the carbonyl groups of Asp-212. Stereoviews of the structure obtained are provided in Figure 7.

Experiments have shown that for the L intermediate the chromophore is indeed more planar than for the K intermediate and that the Schiff base moves closer to its new counterion (Mathies et al., 1991). However, the dramatic rotation of retinal in the BR protein matrix is quite unexpected, and it is doubtful whether such a drastic motion really occurs in the BR photocycle.

The 13-cis → all-trans Reisomerization

The thermal reisomerization of 13-cis-retinal back to the all-trans geometry occurs in the N₅₂₀ → O₆₄₀ transition. In the N intermediate, retinal is reprotonated from Asp-96, and a protein conformational change has probably already occurred (Fodor et al., 1988a). In spite of the fact that MD simulations do not realistically describe protein conformational changes and retinal isomerizations, except if they occur on a very short time scale, we consider it valuable to investigate whether the reprotonated retinal spontaneously undergoes a 13-cis → all-trans isomerization when the barriers are sufficiently lowered such that the process occurs sufficiently fast.

The 13-cis → all-trans isomerization requires crossing over a torsional energy barrier of about 20 kcal/mol and is observed to occur within 5 ms (Lozier et al., 1975). In order for this reaction to be described on a picosecond time scale by an MD simulation, we need to lower the torsional energy barrier for the 13–14 double bond. The structure obtained from simulation B1, in which retinal is deprotonated and in a 13-cis geometry, was used as the initial structure. Retinal partial charges and torsional potential functions were changed to those of the protonated state. In accordance with FTIR data for the N intermediate (Gerwert et al., 1990), Asp-96 was deprotonated (the proton was transferred to the Schiff base), Asp-85 remained protonated, and Asp-212 was deprotonated.

In a first simulation, referred to as D1, the internal torsional barrier for the 13–14 double bond was eliminated by a choice of $k_{\text{dih}} = 0$ in eq 1. Figure 8a presents the dihedral angle trajectory of simulation D1. A torsion of approximately 100° is seen to develop around the 13–14 bond. This torsion allows the Schiff base to form hydrogen bonds with the main chain oxygen atoms of Val-49 and Thr-89, which move closer to the Schiff base and are no longer hydrogen bonded to their original hydrogen-bond donors (NH groups of Ala-53 and Leu-93). The resulting retinal conformation is neither 13-cis nor 13-trans and is clearly unstable in reality due to the 20 kcal/mol torsional potential barrier of the 13–14 bond in the protonated retinal Schiff base.

In a second simulation, referred to as D2, the effect of the two main chain oxygen atoms Val-49 and Thr-89 was decreased by constraining the distance between these two atoms and their original hydrogen-bond donors. Figure 8b shows the resulting time dependence of the dihedral angles of the 13–14, 14–15, and 15–N bonds. The torsion around the 13–14 bond is found to be more complete in simulation D2 compared with that of simulation D1 and the dihedral angle for the bond is stable at around 140°, corresponding to a twisted all-trans structure.

An analysis of simulations D1 and D2 shows that the transition state of the 13-cis → all-trans isomerization, with

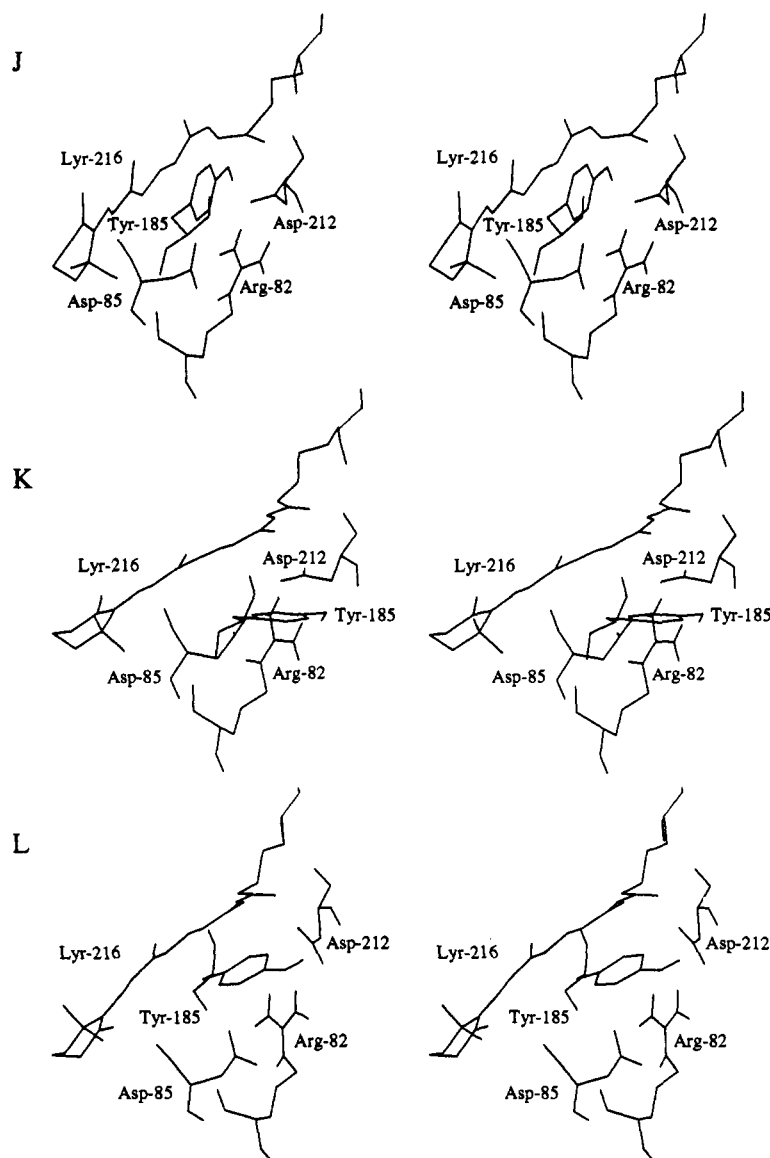


FIGURE 7: Stereoviews of retinal in the putative J, K, and L intermediates obtained from a reaction pathway following an enforced 13-cis photoisomerization in simulation C1 and C2. Neighboring residues Asp-85, Arg-82, Asp-212, and Tyr-185 are also shown.

the dihedral angle of the 13–14 bond approximately at 90° , is stabilized by the main chain oxygen atoms of Val-49 and Thr-89. The potential which governs the reisomerization of retinal from 13-cis to 13-trans in the protein is mainly the sum of two contributions: (1) the internal torsional potential of the 13–14 bond which has a maximum of about 20 kcal/mol at 90° and (2) the interaction potential with the main chain oxygen atoms of Val-49 and Thr-89 which has a minimum at approximately 90° of about 7.4 kcal/mol below the potential value at 0° . The barrier ensuing from the combined contributions is about $(20 - 7.4)$ kcal/mol = 13.6 kcal/mol, which is too high for an isomerization event to occur on the time scale covered by molecular dynamics simulations. We have turned this calamity into an interesting computational experiment by choosing in simulation D3 a barrier for the torsional potential (eq 1) which is about as large as the stabilization through the main chain oxygen atoms of Val-49 and Thr-89, namely, only 7.4 kcal/mol. The ensuing total potential (torsional potential of eq 1 plus protein interactions) should have a very low barrier at 90° because of a cancellation of the internal torsional barrier and external stabilization. Therefore, one would expect that the isomerization 13-cis \rightarrow 13-trans should proceed spontaneously in a respective sim-

ulation. This is, in fact, what we observed: in simulation D3 the isomerization occurred within 1.2 ps through the transition state presented in Figure 9, which is similar to the structure obtained in simulation D1. Figure 8c shows the time dependence of the dihedral angles of the 13–14, 14–15, and 15–N bonds of simulation D3.

Retinal Isomerization Reactions in Structures with Internal Water Structure

The structure resulting when water molecules are placed in the proton conduction channel of BR and the protein is equilibrated is shown in Figure 10a. The distances from the closest atom of Asp-85 and Asp-212 to the Schiff base proton are 3.5 and 3.8 Å, respectively, which agrees well with the Henderson model. Two water molecules are directly hydrogen bonded to the Schiff base. Asp-85, Asp-212, Arg-82, and Thr-89 also participate in hydrogen bonding with these two water molecules. It is interesting that the water molecules are found to be in direct contact with the Schiff base, an arrangement which is consistent with previous suggestions. Such an arrangement of the Schiff base counterion has also been suggested recently by Dér et al. (1991) to explain the chloride pumping activity of BR under low-pH conditions.

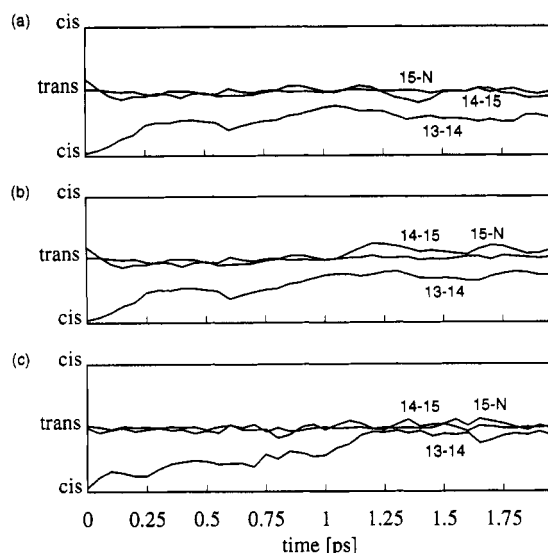


FIGURE 8: Dihedral angles (designated by their respective bonds) of retinal during simulation D1, D2, and D3. The torsional barrier of the 13–14 bond is taken as 0 kcal/mol in simulations D1 and D2 and as 7.4 kcal/mol in simulation D3. The distances between the main chain oxygen atoms of Val-49 and Thr-89 and their original hydrogen-bond donors are constrained in simulation D2.

Another interesting structural and functional motif is a water chain formed on the cytoplasmic side between the hydroxyl group of protonated Asp-96 and the main chain oxygen atom of Lyr-216. Three water molecules participate in forming the chain by hydrogen bonding to each other and the protein polar groups. The chain was found not to be very stable during a total equilibration period of 80 ps.

Photoisomerization. We induced the photoisomerization of retinal in simulation E1 and E2 using the same torsional potential (eq 2) and potential (eq 3) as in simulation A1 and A2, but with internal water in place. The simulations were carried out for 20 ps. Retinal's all-trans \rightarrow 13,14-dicis isomerizations were found to occur within 500 fs in both simulations, as shown by the time dependence of the dihedral angles presented in Figure 11a,b.

One might suspect that since the Schiff base is directly hydrogen bonded to water molecules, the electrostatic forces acting on the retinal Schiff base might be weakened and an all-trans \rightarrow 13-cis photo-isomerization might be favored. This is not the case. The tighter packing of retinal by internal water molecules, in fact, favors an all-trans \rightarrow 13,14-dicis isomerization reaction, as indicated by the occurrence of the isomerization even in case of a 10 kcal/mol energy barrier of the 14–15 bond. A view of the resulting photoproduct is given in Figure 10b. The isomerization is accompanied by a shift of the retinal C₁₀–C₁₅ atoms toward the cytoplasmic side.

The 13,14-dicis \rightarrow 13-cis Reaction Pathway. To study the behavior of retinal upon deprotonation, the structure resulting from simulation E1 was used as a starting point. The protein was modified by deprotonating retinal and protonating Asp-85, and the subsequent dynamics was determined for 40 ps in simulation F1.

Two interesting phenomena were noticed in this simulation. First, retinal undergoes a 13,14-dicis \rightarrow 13-cis isomerization after 3 ps of simulation, as shown in Figure 11c. The isomerization reaction is slower compared to the reaction when no internal water was included (cf. Figure 5). Second, after 5 ps of simulation, the water molecules in the cytoplasmic side of the proton conduction channel change their orientation such that the Schiff base nitrogen becomes the proton acceptor

on one end of the chain. Asp-96, which is protonated, provides the proton donor on the other end of the chain, and a hydrogen-bonded chain is formed. The hydrogen bonding between water molecules and Asp-96 can either be direct or be mediated by the hydroxyl group of Thr-46. A snapshot of the functionally important groups after 20 ps of simulation is given in Figure 12a.

Following simulation F1 we deprotonated Asp-96 and reprotonated the Schiff base, according to the proton transfer observed in the M₄₁₂ \rightarrow N₅₂₀ transition. The subsequent dynamics was determined for 20 ps (simulation F2). The direction of the water chain in the upper channel is reversed through rotation of all water molecules, and the chain is partially deformed, as shown in Figure 12b.

Subsequent to simulation F2, Asp-96 was reprotonated and Asp-85 deprotonated again in an attempt to simulate the N \rightarrow BR₅₆₈ transition in the presence of the internal water molecules. We decreased the torsional barrier of retinal's 13–14 bond to 0 kcal/mol and carried out a corresponding simulation F3 for 40 ps. Retinal remained in the 13-cis geometry during the simulation due to the strong attraction between the protonated Schiff base and the water molecules in the upper part of the proton conducting channel. Therefore, the 13-cis \rightarrow all-trans reisomerization was not realized in the simulations when water is present in the upper proton conducting channel.

The Enforced 13-cis Reaction Pathway. An enforced 13-cis photoisomerization reaction was induced for the structure of BR with internal water in simulation G1. For k_{dih}^{13} (cf. eq 2) a value of 47 kcal/mol (eq 2) was assumed (corresponding to an initial energy storage of 94 kcal/mol in the excited state), and for k_{dih}^{14} (cf. eq 3) a value of 10 kcal/mol was assumed (corresponding to a torsional barrier of 20.0 kcal/mol for the 14–15 bond). The latter value is twice as large as that chosen in simulation C1 since in the presence of water a lower barrier of 10 kcal/mol does not prevent a rotation of the 14–15 bond in the photoisomerization step (cf. Figure 11b). The corresponding simulation G1 was carried out for 6 ps.

A 13-cis isomerization reaction was found to occur within 200 fs (not shown). The Schiff base proton and the water molecules hydrogen bonded to it moved very little during this reaction. The 14–15 bond and the retinal plane became highly twisted. After 600 fs, the Schiff base proton was no longer hydrogen bonded to Asp-85 or Asp-212, but instead hydrogen bonded to Thr-89 through a water molecule as shown in Figure 13a. This photoproduct is unstable and would relax back to the all-trans geometry if the ground state torsional potential of retinal would be reinstated at this time as test simulations revealed.

During the further course of simulation G1, retinal and the surrounding protein, still under the constraints of the photoisomerization potential (eq 2), equilibrated: the Schiff base proton moved toward the cytoplasmic side and the twist in the retinal plane decreased, retinal remained hydrogen bonded to Thr-89 through a water molecule, another water molecule in the cytoplasmic side of the proton channel also became hydrogen bonded to the Schiff base, and the water chain of the initial Br₅₆₈ form (cf. Figure 10a) was deformed. The conformations of important residues at this stage of simulation G1 are shown in Figure 13b. After completion of simulation G1, i.e., after 6 ps, the 13-cis intermediate is stable. In fact, a subsequent 70-ps simulation G2, reinstating the ground state torsional potential of retinal, did not give rise to any major alteration of retinal's geometry.

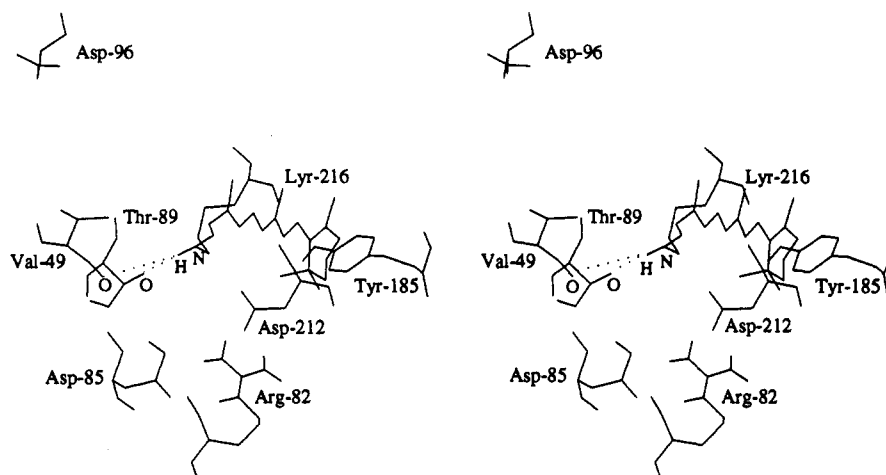


FIGURE 9: Stereoview of the geometry of retinal in the transition state of the 13-cis \rightarrow all-trans isomerization in simulation D3. The Schiff base forms hydrogen bonds with the main chain oxygen atoms of Val-49 and Thr-89, and, accordingly, the transition state is stabilized.

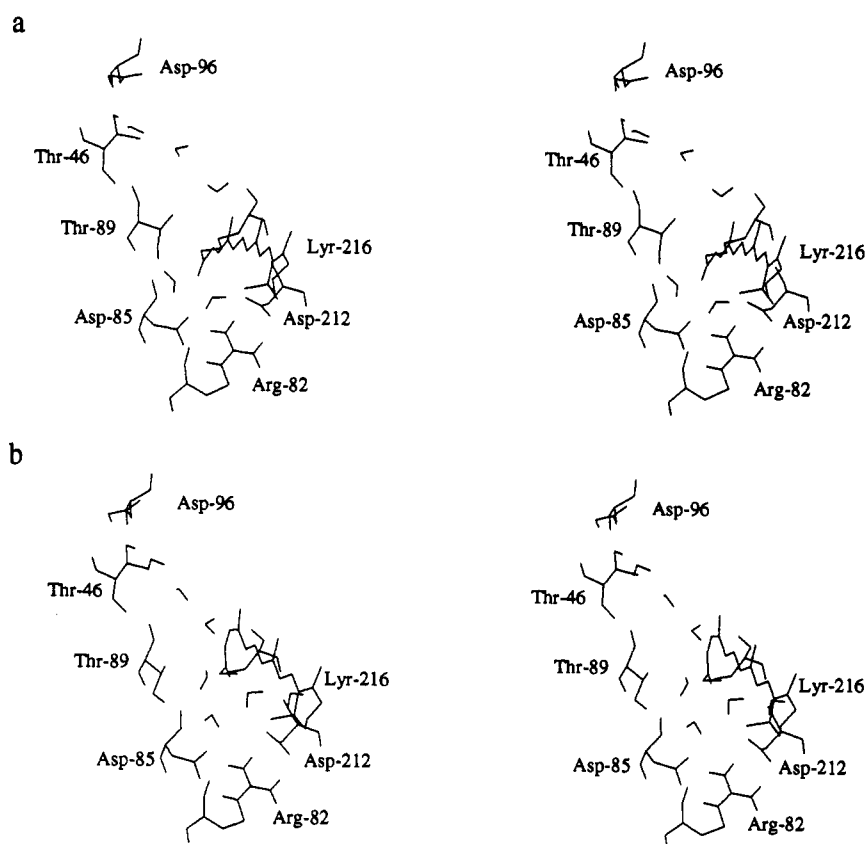


FIGURE 10: (a) Stereoview of the BR structure with internal water molecules. Retinal, protein residues directly involved in the proton pumping, and water molecules close to retinal are shown. (b) BR structure after the induced retinal photoisomerization. The Schiff base is hydrogen bonded to Asp-85 and Asp-212 via water molecules.

The structure resulting from simulation G2 is presented in Figure 13c. Retinal became further geometrically relaxed as judged by the decrease of the twist of the chromophore backbone. A chain of three water molecules is formed between the Schiff base proton and Asp-85 after about 50 ps of simulation. The direction of retinal's plane slightly rotated away from the membrane normal and the Schiff base as well as the C₁₀–C₁₅ atoms moved toward the cytoplasmic side as compared to the structure before photoisomerization.

Simulation G3 continued simulation G2, albeit for a deprotonated Schiff base and a protonated Asp-85. The simulation lasted 40 ps. After deprotonation, retinal became very flexible and the stress in the chromophore was released. The water chain between the Schiff base and Asp-85 deformed.

The water chain which was established in simulation F1 connecting Asp-96 to the unprotonated retinal was not formed in simulation G3 during 40 ps (not shown), although it could be formed in principle since the protonation state of the protein is identical to that in simulation F1.

DISCUSSION

Role of the Schiff Base–Counterion Interaction in the Photocycle. It has been suggested that the reaction processes of the bacteriorhodopsin photocycle are driven mainly by steric interactions at short times (~ 1 ns), by electrostatic interactions at medium times (~ 1 μ s), and by entropic interactions at long times (~ 1 ms) (Schulten et al., 1984). We have shown in the present work that electrostatic and steric interactions

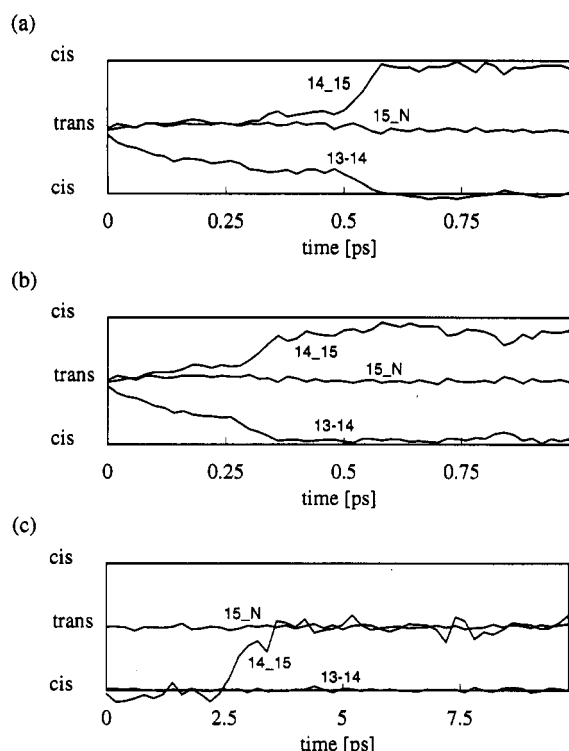


FIGURE 11: Dihedral angle trajectories of retinal isomerization reactions. (a) The 13,14-dicis photoisomerization in simulation E1 in which a torsional barrier for the 14–15 bond of 10 kcal/mol has been assumed. (b) The 13,14-dicis photoisomerization in simulation E2 in which a torsional barrier for the 14–15 bond of 2 kcal/mol has been assumed. (c) The 13,14-dicis \rightarrow 13-cis isomerization induced by retinal deprotonation in simulation F1.

control both the early part of the photocycle and most likely also the later part. The electrostatic interaction between the Schiff base and its counterion has been found to be extremely important in determining retinal's geometry in the primary photoisomerization for both the 13,14-dicis and the 13-cis isomerization models investigated.

In our simulations, the position of the Schiff base proton remains largely unchanged during the photoisomerization because of the Schiff base-counterion interaction. Since the β -ionone ring of retinal is tightly packed in the protein matrix and has a relatively large mass, it too is not subject to large motion. Therefore, only the molecular moiety between the Schiff base and the β -ionone ring can move during the primary photoreaction. A likely motion is the simultaneous rotation of the 13–14 and 14–15 bonds, a motion which can occur without intolerable twist of retinal's backbone, whereas rotation of the 13–14 bond alone is sterically unfavorable.

While it is clear from the present investigation that the flexible lysine side chain can easily adapt to the large conformational change occurring during a 13-cis isomerization, such adaptation is not sufficient to enable retinal to undergo such an isomerization during the primary photoreaction. Whether a 13-cis or a 13,14-dicis isomerization should occur depends on the torsional barrier of the 14–15 bond in the photoreaction and on the detailed nature of the Schiff base counterion. Internal water molecules, which participate in forming the proton accepting complex, can also affect the nature of the primary photoisomerization. Unfortunately, a high-resolution structure of BR is required to identify water molecules in retinal's binding site. Quantum chemical calculations of retinal in the excited state [for a review, see (Birge, 1990)] would be desirable to describe the behavior of the 14–15 bond during the primary isomerization reaction.

Our simulations have shown that a 13-cis photoproduct can be enforced through an extreme potential (depositing 94 kcal/mol in the initial excited state), but the resulting retinal isomer can not be stabilized within about 3 ps since the binding site does not accommodate the 13-cis geometry properly. This result supports the suggestion that a 13-cis photoproduct would revert back to BR since the low 13–14 torsional barrier of protonated Schiff base retinal is not high enough to store energy (~ 15 kcal/mol) in the primary intermediate (Schulten et al., 1984). A 13,14-dicis photoproduct, on the other hand, is stable, because of the high barrier of a thermal 13,14-dicis \rightarrow all-trans isomerization and because 13,14-dicis retinal can be accommodated well by the binding site.

Upon deprotonation retinal spontaneously undergoes a 13,14-dicis \rightarrow 13-cis isomerization in MD simulations. It was previously suggested that a 13,14-dicis \rightarrow 13-cis isomerization can occur in the $L_{550} \rightarrow M_{412}$ transition because the barrier of rotation around the 14–15 bond is lowered to only a few kcal/mol by deprotonation of the Schiff base (Schulten et al., 1984; Tavan et al., 1985). The present investigation suggests that such an isomerization, in addition, is facilitated by the change in electrostatic interaction between the Schiff base and its counterion caused by retinal's deprotonation. Deprotonation removes the attraction between the Schiff base and its counterion, enables retinal to quickly rotate around the 14–15 bond, and thereby releases the high intramolecular energy stored in the 13,14-dicis geometry (Orlandi & Schulten, 1979).

This 13,14-dicis \rightarrow 13-cis isomerization rotates the Schiff base nitrogen away from the proton acceptor (assumed to be Asp-85) to face the cytoplasmic side, such that retinal is ready to be reprotonated from Asp-96. The isomerization is completed within 700 fs when no internal water is included and is completed within 2.5 ps when internal water molecules are placed in the retinal binding pocket. The reaction times indicate that the isomerization occurs very fast. Thus, a deprotonated 13,14-dicis retinal should not be observable experimentally, although a higher torsional barrier for the 14–15 single bond than that used in our simulation (2 kcal/mol) could increase the time needed for this isomerization. We suggest that the 13,14-dicis \rightarrow 13-cis isomerization might be coupled to retinal deprotonation in the $L_{550} \rightarrow M_{412}$ transition, causing the free energy change of this transition to be close to zero, in agreement with experimental results (Váró & Lanyi, 1991a,b). Thus, the geometry of retinal would be 13-cis in the M state, leaving the experimentally distinguished M_1 and M_2 intermediates to be explained by subsequent conformational changes of the protein or by a transition in the geometry of internally bound water.

While retinal undergoes a 13-cis \rightarrow all-trans isomerization upon reprotonation in simulations which do not include internal water, such a reaction does not proceed spontaneously within the simulation periods when water molecules are added. The reaction could be catalyzed by neutralizing or removing a negative counterion from the Schiff base proton (Tavan et al., 1985; Baasov & Sheves, 1984b) as well as by properly placed anionic groups which can lower the torsional barrier of the 13–14 bond, as suggested by some theoretical studies (Tavan et al., 1985; Seltzer, 1987). The catalytic mechanism involving the Val-49 and Thr-89 main chain oxygens, discussed under Results, invites the following critique. First, the protein conformation in N could be different from the structure we generated by MD simulation. Second, the protonation state of the N intermediate and the structure of internal water molecules might differ from what has been assumed in our

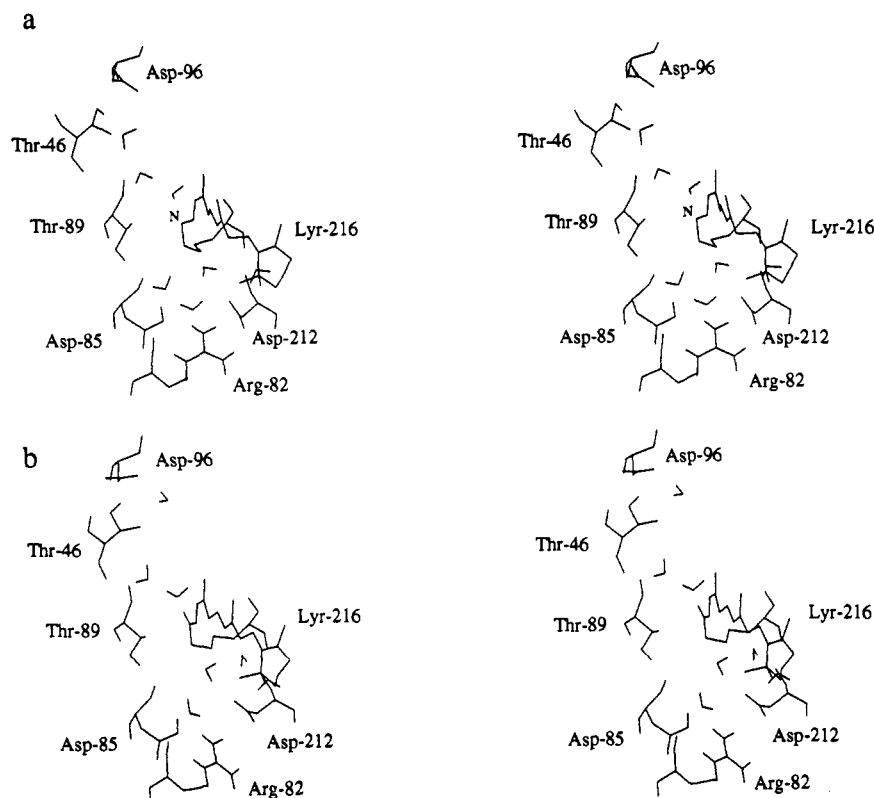


FIGURE 12: BR structure after retinal's deprotonation (top) and reprotonation (bottom). Retinal undergoes a 13,14-dicis \rightarrow 13-cis isomerization after deprotonation, and a water chain provides a "proton wire" between Asp-96 and the Schiff base nitrogen. Since there is no Schiff base proton in panel a, we have denoted the position of the Schiff base nitrogen by "N".

simulations. In reality, this isomerization reaction is intercepted by the O_{640} intermediate, the nature of which is not well understood. Protonation state changes of Asp-212 and, possibly, of Arg-82 are suggested to be involved in the $N_{520} \rightarrow O_{640}$ and $O_{640} \rightarrow BR_{568}$ transitions, and this is not accounted for in our simulations.

Since the electrostatic interactions between the retinal Schiff base and the protein environment are shown in this study to be a crucial factor for the retinal isomerization reactions, a realistic description of these interactions in the molecular modeling is very important. Accurate partial charges assigned to the retinal atoms and proper treatment of the hydrogen-bonding interactions and the protein polarization effect would be required to describe the electrostatic interactions quantitatively. For example, using a dielectric constant of 2.0 instead of 1.0 would decrease all the interaction energies. In the present study, the partial charges assigned to the retinal Schiff base are somewhat larger than the charges found in a few other modeling studies (Tavan et al., 1985; Birge et al., 1987), and the dielectric constant used is 1.0. This might lead to an overestimate of the electrostatic interactions in the protein, although it is difficult to determine at the present stage how large this effect would be. It is probably not an easy task to describe the electrostatic interactions in BR accurately without extensive calculations and calibrations with experimental facts, which awaits more theoretical and experimental studies in the future.

Our simulations do not yield an obvious explanation for the nature of the O_{640} intermediate. Likely explanations are a proton transfer from Arg-82 to Asp-212 and the observed protonation of Asp-85, which both should contribute to the strong spectral red-shift of this intermediate. Another contribution distinguishing this intermediate from BR_{568} could be properly oriented water molecules. Since our simulations enforced the completion of the whole pump cycle on a 100-ps

time scale, we could not expect that the difference between BR_{568} and O_{640} , which, save for a possible torsion of retinal, must be due to the protein matrix, could reveal itself. More extended simulations describing longer time scales and also describing charge shifts in the protein will be required to account for the BR_{568} – O_{640} difference.

Comparison of the 13,14-dicis and 13-cis Isomerization Models. The results of the present study show that the behavior of retinal is consistent with the 13,14-dicis isomerization model of BR function. Figure 14 presents the complete sequence of isomerizations and proton transfers consistent with that model. After the photoisomerization, shown as the first step in Figure 14, retinal is in a 13,14-dicis geometry. Deprotonation of retinal releases the Schiff base nitrogen from its counterion, and the barrier of rotation around the 14-15 bond is lowered to a few kcal/mol (Schulten et al., 1984; Tavan et al., 1985). Retinal, accordingly, isomerizes to the 13-cis state presented as the second step in Figure 14. In fact, the high intramolecular energy stored in 13,14-dicis retinal decreases the pK value of the Schiff base and facilitates the transfer of the Schiff base proton to Asp-85 (Schulten, 1978; Tavan et al., 1985). However, the barrier for rotation around the 13–14 bond is over 40 kcal/mol in the unprotonated retinal (Tavan et al., 1984), and the system stays in the 13-cis geometry in the M intermediate. Protonation of retinal in the N intermediate enables the thermal reisomerization reaction to occur and brings the system back to BR_{568} , shown as the third step in Figure 14. Changes in retinal's torsional potentials as well as changes in the retinal–protein electrostatic interactions control the proton pump cycle.

Although our simulations indicate that a 13-cis photoisomerization is unfavorable in BR as compared to a 13,14-dicis photoisomerization, the possibility of a 13-cis photoisomerization as a first step in the pump cycle may not be excluded. Simulations show that internal water molecules

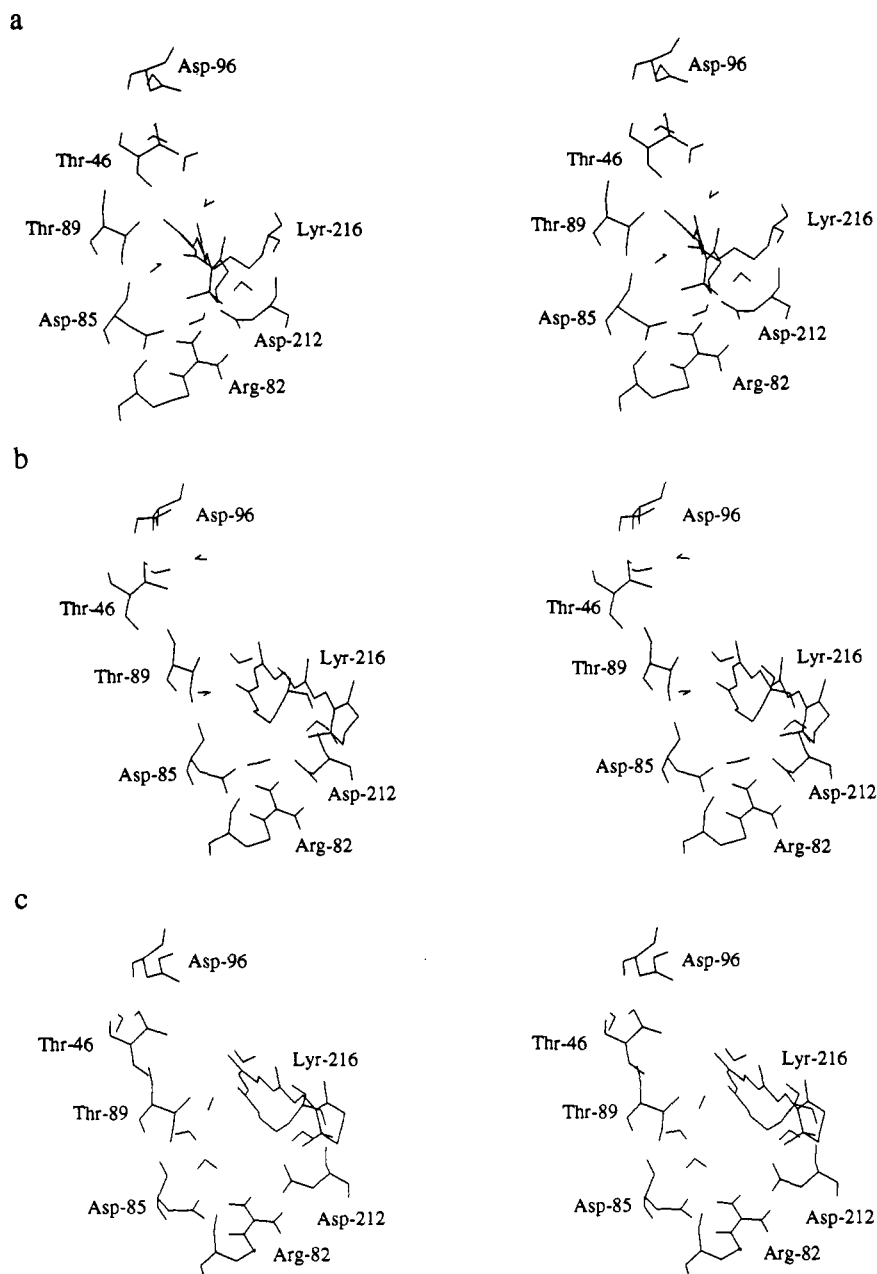


FIGURE 13: BR structure after the enforced 13-cis isomerization. (a) 600 fs after the isomerization; (b) 3 ps after the isomerization; (c) 70 ps after the isomerization.

have significant effects on the 13-cis photoisomerization. When water molecules are absent, retinal rotates violently to maintain the Schiff base-counterion interaction. When water molecules are present, they serve as primary counterions and retinal can be stabilized without such a rotation. After the 13-cis isomerization, retinal first forms a hydrogen bond to Thr-89 via water molecules and then forms a hydrogen bond to Asp-85 through a water chain, which should enable the proton transfer from retinal to Asp-85 in the $L_{550} \rightarrow M_{412}$ transition. In a recent paper, it was reported that Thr-89 is involved in a transient hydrogen-bond network, and mutations of this residue affect the formation of the K intermediate (Rothschild et al., 1992). Deformation of the hydrogen-bonded chain originally formed by Asp-96, Thr-46, and three water molecules after the 13-cis isomerization may also explain the changes in the FTIR spectra of Asp-96 in the L intermediate. Although not shown in our simulations, this hydrogen-bonded chain, in principle, could be re-formed and be stabilized when retinal is deprotonated, connecting Asp-96, which is protonated

at this stage, to the Schiff base nitrogen which has a negative partial charge.

Although the two models of the pump cycle of BR described above are very different, they are quite similar in terms of the roles of electrostatic and steric interactions in controlling the cycle, as shown in the reaction scheme presented in Figure 15. Retinal isomerizes after absorbing light and is still hydrogen bonded to the primary counterion Asp-85 through a water molecule or through a water chain. The structure is electrostatically favored because of the positive charge on the Schiff base and the negative charge on Asp-85. To maintain such a configuration, steric energy is stored in retinal and the pK_a value of the Schiff base is lowered. After the deprotonation of retinal, the steric energy in retinal is released either by a 13,14-dicis \rightarrow 13-cis isomerization or by a relaxation of 13-cis retinal. A water chain similar to one also found in gramicidin A (Cao et al., 1991) is formed between the proton of Asp-96 and the Schiff base nitrogen. The chain is also electrostatically favored because of the partial charges of the protein atoms

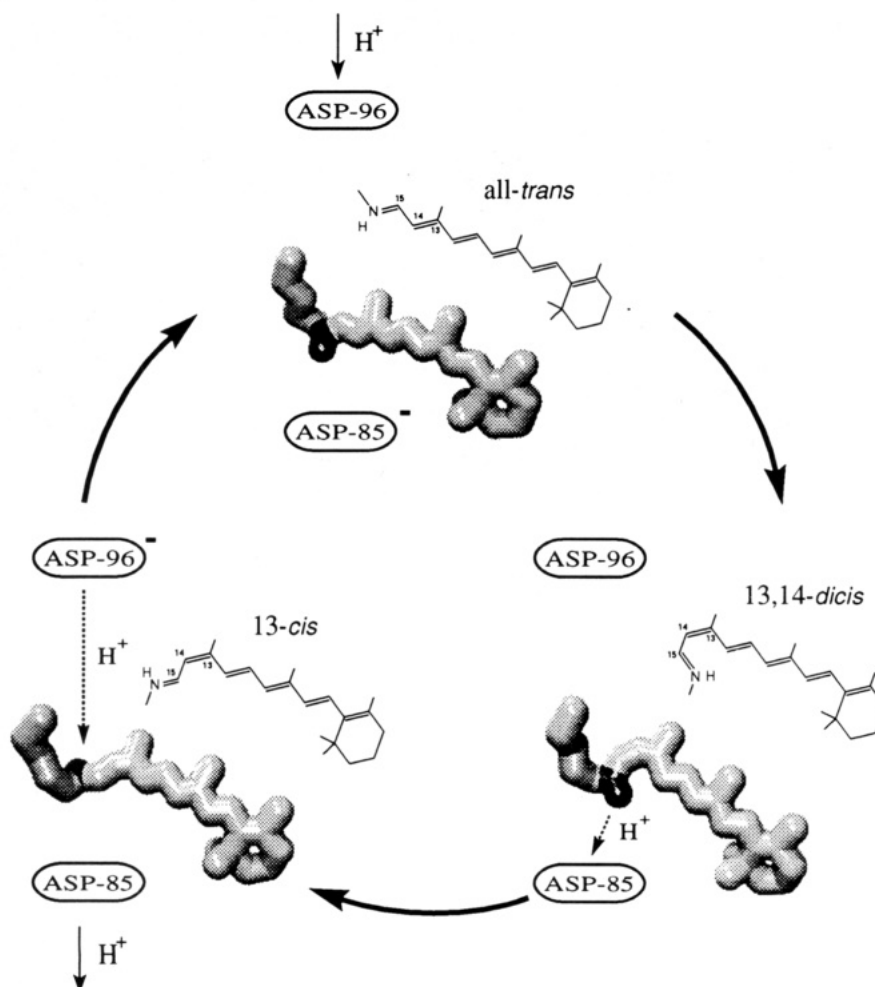


FIGURE 14: Isomerization states of retinal during the photocycle according to the 13,14-dicis isomerization model. Retinal first undergoes an all-trans to 13,14-dicis photoisomerization. The Schiff base proton is pointing (down) toward the extracellular side, being held there by the electrostatic interaction to its counterion. After the proton is transferred to the primary proton acceptor Asp-85, retinal releases some of its internal energy through an isomerization which leads to a 13-cis geometry. The Schiff base is turned around, brought closer to the primary proton donor Asp-96, and re-protonated from there. After reprotonation, retinal reisomerizes back to the all-trans state and completes the photocycle.

on the two ends. Retinal then reprotonates from Asp-96 through this chain. Reprotonation of Asp-96 is required in the $N_{520} \rightarrow O_{640}$ transition (Váró & Lanyi, 1990; Cao et al., 1991), probably because reprotonation of Asp-96 brings in a defect of this hydrogen-bonded chain and destabilizes the 13-cis protonated retinal, thereby decreasing the activation energy of retinal's reisomerization reaction. It thus appears that hydrogen-bonded chains formed by water molecules between positively and negatively charged protein atoms are very important in the BR proton pump cycle.

Photoelectric observations suggest that a charge separation in a direction opposite to that of the net proton transfer occurs within 20 ps after photon absorption in both hydrated and dehydrated BR (Keszthelyi & Ormos, 1980; Trissl, 1990). In our simulations, the charge separation is mainly due to the movement of the retinal C_{10} – C_{15} atoms, which have positive partial charges, toward the cytoplasmic side of the protein. Since both a 13-cis and a 13,14-dicis photoisomerization involve similar movements of these atoms, the charge separation should occur in both cases. Therefore, the observed charge transfer does not allow one to discriminate between the two primary photoisomerizations.

Importance of Molecular Dynamics in Understanding the Mechanism of Bacteriorhodopsin. The studies of the isomerization reactions in the BR proton pump cycle presented above demonstrate how molecular dynamics investigations can be

exploited for a better understanding of the functional details of basic biochemical reactions. One of the interesting aspects of the MD simulations of retinal's isomerizations in bacteriorhodopsin is that the isomers tend to look quite different from the ideal geometries implied by terms like "all-trans", "13-cis", etc. The simulations revealed that many degrees of freedom (bond and torsion angles) participate in the photoisomerization reaction of retinal. Although each individual bond and torsion angle differs only little from the ideal configuration, the shape of retinal can look much different from what one expects assuming ideal geometries.

Figure 14 illustrates this aspect using the configurations from our model for the photocycle as an example. In the case of the 13,14-dicis isomerization, it turns out that the Schiff base proton moves very little, which was not expected when the 13,14-dicis isomerization model was first proposed in (Schulten, 1978). This lack of movement allows the proton to stay close to the counterion to which it is attracted electrostatically. Only a slight tilt in the whole chromophore is necessary to balance the resulting nonideal configuration. Only MD simulations of the complete system including protein and chromophore can hope to describe such effects correctly.

The present simulations are based on the Henderson structure, which is not of high resolution. There is experimental support for both Asp-85 and Asp-212 as the primary counterion of the Schiff base (Lin & Mathies, 1989; Otto et

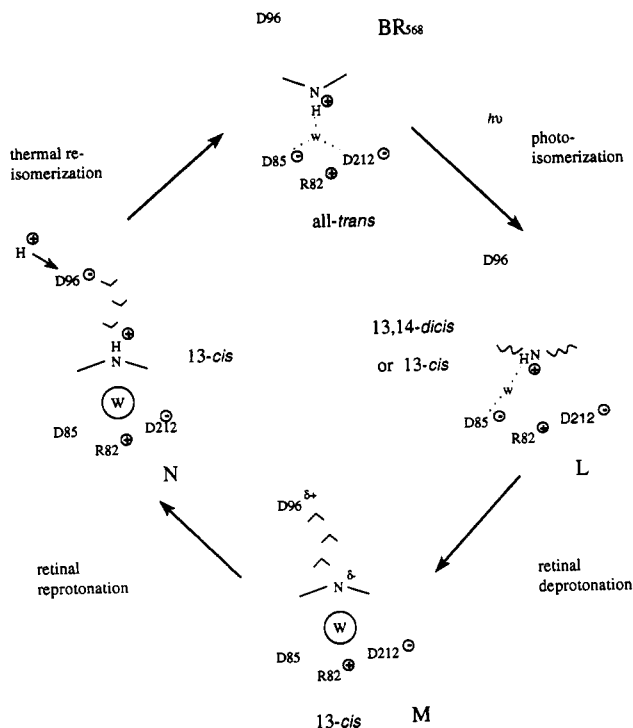


FIGURE 15: Schematic model of the BR photocycle controlled by electrostatic interactions and steric interactions. Formation of hydrogen-bonded chains between positive (partial) charges and negative (partial) charges is considered very important in determining structures of the intermediates and in carrying out the proton pumping function. Partial charges of protein atoms are denoted as δ^+ or δ^- . Steric stress of retinal is shown by drawing retinal in curved lines.

al., 1990; Subramaniam et al., 1990). The exact role of water molecules in the proton-accepting complex is also not clear. Simulations in the present study, however, have shown that the primary photoreaction and also later reactions in the photocycle are affected by the retinal-protein electrostatic interaction, which is sensitive to the arrangement of charged protein groups and water molecules around the Schiff base. In order to determine the detailed mechanism of proton pumping in BR, higher resolution structures with better identification of water molecules and specific hydrogen bonds would be needed. Placement of water molecules and accurate calculations of the electrostatic field inside the protein will also be required to describe the pK values of groups involved in the proton conduction pathway and controlling the protonation state of the retinal chromophore. Since high-resolution structures for BR intermediates will not be available for a long time, MD simulations will have to fill in the remaining information. The present study serves as a first attempt to describe the complete photocycle using simulation techniques.

ACKNOWLEDGMENT

We thank Marco Nonella for the topology file of Lyr-216 and for the partial charges of protonated and unprotonated retinal. Simulations in an early exploratory phase were accomplished on a Transputer-based computer operated by the Resource for Computational Biology at the University of Illinois and on a Connection Machine CM-2. Some of the simulations were carried out on a Cray 2. The latter two machines are operated by the National Center for Supercomputing Applications funded by the National Science Foundation. We also thank Prof. Modechai Sheves for helpful discussions in revising the manuscript.

REFERENCES

- Aton, B., Doukas, A. G., Callender, R. H., Becker, B., & Ebrey, T. G. (1977) *Biochemistry* 16, 2995–2999.
- Baasov, T., & Sheves, M. (1984a) *Angew. Chem.* 96, 786–787.
- Baasov, T., & Sheves, M. (1984b) *J. Am. Chem. Soc.* 106, 6840–6841.
- Baasov, T., & Sheves, M. (1985) *J. Am. Chem. Soc.* 107, 7524–7533.
- Baasov, T., & Sheves, M. (1986) *Biochemistry* 25, 5249–5258.
- Bashford, D., & Gerwert, K. (1992) *J. Mol. Biol.* 224, 473–486.
- Becher, B. F. T., & Ebrey, T. G. (1978) *Biochemistry* 17, 2293–2300.
- Birge, R. (1990) *Annu. Rev. Phys. Chem.* 41, 683–733.
- Birge, R. R., Murray, L. P., Zidovetzki, R., & Knapp, H. M. (1987) *J. Am. Chem. Soc.* 109, 2090–2101.
- Braiman, M. S., Ahl, P., & Rothschild, K. J. (1987) *Proc. Natl. Acad. Sci. U.S.A.* 84, 5221–5225.
- Braiman, M. S., Mogi, T., Marti, T., Stern, L. J., Khorana, H. G., & Rothschild, K. J. (1988) *Biochemistry* 27, 8516–8520.
- Brooks, B. R., Bruccoleri, R. E., Olafson, B. D., States, D. J., Swaminathan, S., & Karplus, M. (1983) *J. Comput. Chem.* 4, 187–217.
- Brünger, A. T. (1988) in *Crystallographic Computing 4: Techniques and New Technologies* (Isaacs, N. W., & Taylor, M. R., Eds.) Clarendon Press, Oxford.
- Cao, Y., Váró, G., Chang, M., Ni, B., Needleman, R., & Lanyi, J. K. (1991) *Biochemistry* 74, 110972–110979.
- de Groot, H., Smith, S., Courtin, J., van den Berg, E., Winkel, C., Lugtenburg, J., Griffin, R., & Herzfeld, J. (1990) *Biochemistry* 29, 6873–6883.
- Dencher, N., Dresselhaus, D., Zaccari, G., & Büldt, G. (1989) *Proc. Natl. Acad. Sci. U.S.A.* 86, 7876–7879.
- Dér, A., Száz, S., Tóth-Boconádi, R., Tokaji, Z., Keszthelyi, L., & Stoeckenius, W. (1991) *Proc. Natl. Acad. Sci. U.S.A.* 88, 4751–4755.
- Dobler, J., Zinth, W., Kaiser, W., & Osterhelt, D. (1988) *Chem. Phys. Lett.* 144, 215–220.
- Engelhard, M., Hess, B., Metz, G., Kreutz, W., Siebert, F., Soppa, J., & Osterhelt, D. (1990) *Eur. Biophys. J.* 18, 17–24.
- Fahmy, K., Siebert, F., Grossjean, M., & Tavan, P. (1989) *J. Mol. Struct.* 214, 257–288.
- Fodor, S. P. A., Ames, J. B., Gebhard, R., van den Berg, E. M. M., Stoeckenius, W., Lugtenburg, J., & Mathies, R. A. (1988a) *Biochemistry* 27, 7097–7101.
- Fodor, S. P. A., Pollard, W. T., Gebhard, R., van den Berg, E. M. M., Lugtenburg, J., & Mathies, R. (1988b) *Proc. Natl. Acad. Sci. U.S.A.* 85, 2156–2160.
- Gat, Y., Grossjean, M., Pinevsky, I., Takei, H., Rothman, Z., Sigrist, H., Lewis, A., & Sheves, M. (1992) *Proc. Natl. Acad. Sci. U.S.A.* 89, 2434–2438.
- Gerwert, K. (1992) *Biochim. Biophys. Acta* 1101, 147–153.
- Gerwert, K., & Siebert, F. (1986) *EMBO J.* 4, 805–812.
- Gerwert, K., & Souvignier, G. (1992) *Biophys. J.* 63, 1393–1405.
- Gerwert, K., Hess, B., Soppa, J., & Osterhelt, D. (1989) *Proc. Natl. Acad. Sci. U.S.A.* 86, 4943–4947.
- Gerwert, K., Souvignier, G., & Hess, B. (1990) *Proc. Natl. Acad. Sci. U.S.A.* 87, 9774–9778.
- Glaeser, R., Baldwin, J., Ceska, T. A., & Henderson, R. (1986) *Biophys. J.* 50, 913–920.
- Grossjean, M., Tavan, P., & Schulten, K. (1989) *Eur. Biophys. J.* 16, 341–349.
- Grossjean, M., Tavan, P., & Schulten, K. (1990) *J. Phys. Chem.* 94, 8059–8069.
- Harbison, G., Smith, S., Pardo, J., Courtin, J., Lugtenburg, J., Herzfeld, J., Mathies, R., & Griffin, R. (1985) *Biochemistry* 24, 6955–6962.
- Henderson, R. (1977) *Annu. Rev. Biochem. Bioeng.* 6, 87–109.
- Henderson, R., Baldwin, J., Ceska, T., Zemlin, F., Beckmann, E., & Downing, K. (1990) *J. Mol. Biol.* 213, 899–929.

- Hildebrandt, P., & Stockburger, M. (1984) *Biochemistry* 23, 5539–5548.
- Holz, M., Drachev, L., Mogi, T., Otto, H., Kaulen, A., Heyn, M., Skulachev, V., & Khorana, H. (1989) *Proc. Natl. Acad. Sci. U.S.A.* 86, 2167–2171.
- Jorgenson, W. L., Chandrasekhar, J., & Madura, J. D. (1983) *J. Chem. Phys.* 79, 926–935.
- Keszthelyi, L., & Ormos, P. (1980) *FEBS Lett.* 109, 189–193.
- Khorana, H. (1988) *J. Biol. Chem.* 263, 7439–7442.
- Kouyama, T., Kouyama, A., Ikegami, A., Mathew, M., & Stoeckenius, W. (1988) *Biochemistry* 27, 5855–5863.
- Lin, S., & Mathies, R. (1989) *Biophys. J.* 56, 653–660.
- Lozier, R. H., Bogomolni, R. A., & Stoeckenius, W. (1975) *Biophys. J.* 15, 955–962.
- Maeda, A., Sasaki, J., Shishida, Y., & Yoshizawa, T. (1992a) *Biochemistry* 31, 462–467.
- Maeda, A., Sasaki, J., Shishida, Y., Yoshizawa, T., Chang, M., Ni, B., Needleman, R., & Lanyi, J. (1992b) *Biochemistry* 31, 4684–4690.
- Mathies, R., Cruz, C., Pollard, W., & Shank, C. (1988) *Science* 240, 777–779.
- Mathies, R., Lin, S., Ames, J., & Pollard, W. (1991) *Annu. Rev. Biophys. Biophys. Chem.* 20, 491–518.
- Mogi, T., Stern, L., Marti, T., Chao, B., & Khorana, H. (1988) *Proc. Natl. Acad. Sci. U.S.A.* 85, 4148–4152.
- Nagle, J. F., & Nagle, S. T. (1983) *J. Membr. Biol.* 74, 1–14.
- Nakanishi, K., Balog-Nair, V., Arnaboldi, M., Tsujimoto, K., & Honig, B. (1980) *J. Am. Chem. Soc.* 102, 7945–7947.
- Needleman, R., Chang, M., Ni, B., Váró, G., Fornes, J., White, S., & Lanyi, J. (1991) *J. Biol. Chem.* 266, 11478–11484.
- Nonella, M., Windemuth, A., & Schulten, K. (1991) *Photochem. Photobiol.* 54, 937–948.
- Oesterhelt, D. (1976) *Angew. Chem., Int. Ed. Engl.* 15, 16–24.
- Oesterhelt, D., & Stoeckenius, W. (1971) *Nature (London), New Biol.* 233, 149–152.
- Oesterhelt, D., & Stoeckenius, W. (1973) *Proc. Natl. Acad. Sci. U.S.A.* 70, 2853–2857.
- Oesterhelt, D., Hegemann, P., Tavan, P., & Schulten, K. (1986) *Eur. Biophys. J.* 14, 123–129.
- Orlandi, G., & Schulten, K. (1979) *Chem. Phys. Lett.* 64, 370–374.
- Otto, H., Marti, T., Holz, M., Mogi, T., Stern, L. J., Engel, F., Khorana, H., & Heyn, M. P. (1990) *Proc. Natl. Acad. Sci. U.S.A.* 87, 1018–1022.
- Papadopoulos, G., Dencher, N., Zaccari, G., & Büldt, G. (1990) *J. Mol. Biol.* 214, 15–19.
- Pettei, M., Yudd, A., Nakanishi, K., Henselman, R., & Stoeckenius, W. (1977) *Biochemistry* 16, 1955–1959.
- Racker, E., & Stoeckenius, W. (1974) *J. Biol. Chem.* 249, 662–663.
- Ridley, J., & Zerner, M. (1973) *Theor. Chim. Acta* 32, 111–134.
- Rothschild, K. J., He, Y. W., Sonar, S., Marti, T., & Khorana, H. G. (1992) *J. Biol. Chem.* 267, 1615–1622.
- Sandorfy, D., & Vocelle, D. (1986) *Can. J. Chem.* 64, 2251–2266.
- Schulten, K. (1978) in *Energetics and Structure of Halophilic Microorganism* (Caplan, S., & Ginzburg M., Eds.) pp 331–334, Elsevier, Amsterdam.
- Schulten, K., & Tavan, P. (1978) *Nature* 272, 85–86.
- Schulten, K., Schulten, Z., & Tavan, P. (1984) in *Information and Energy Transduction in Biological Membranes* (Bolis, L., Helmreich, E., & Passow, H., Eds.) pp 113–131, Alan R. Liss, New York.
- Seltzer, S. (1987) *J. Am. Chem. Soc.* 109, 1627–1631.
- Smith, S., Pardo, J., Mulder, P., Curry, B., & Lugtenburg, J. (1983) *Biochemistry* 22, 6141–6148.
- Smith, S., Hornung, I., van der Steen, R., Pardo, J., Braiman, M., Lugtenburg, J., & Mathies, R. (1986) *Proc. Natl. Acad. Sci. U.S.A.* 83, 967–971.
- Subramaniam, S., Marti, T., & Khorana, H. G. (1990) *Proc. Natl. Acad. Sci. U.S.A.* 87, 1013–1017.
- Tavan, P., Schulten, K., & Osterhelt, D. (1985) *Biophys. J.* 47, 415–430.
- Trissl, H. (1990) *Photochem. Photobiol.* 51, 793–818.
- Váró, G., & Keszthelyi, L. (1983) *Biophys. J.* 43, 47–51.
- Váró, G., & Lanyi, J. K. (1990) *Biochemistry* 29, 6858–6865.
- Váró, G., & Lanyi, J. K. (1991a) *Biochemistry* 30, 5016–5022.
- Váró, G., & Lanyi, J. K. (1991b) *Biochemistry* 30, 5008–5015.
- Warshel, A., & Barboy, N. (1982) *J. Am. Chem. Soc.* 104, 1469–1476.
- Zhukovsky, E., Robinson, P., & Oprian, D. (1991) *Science* 251, 558–560.